Article

Elucidating Amyloid β-Protein Folding and Assembly: A Multidisciplinary Approach

David B. Teplow, Noel D. Lazo, Gal Bitan, Summer Bernstein, Thomas Wyttenbach, Michael T. Bowers, Andrij Baumketner, Joan-Emma Shea, Brigita Urbanc, Luis Cruz, Jose Borreguero, and H. Eugene Stanley

Acc. Chem. Res., **2006**, 39 (9), 635-645• DOI: 10.1021/ar050063s • Publication Date (Web): 22 July 2006

Acc. Chem. Res. **2006,** *39,* 635−645

Elucidating Amyloid β-Protein Folding and Assembly: A Multidisciplinary Approach

DAVID B. TEPLOW,*,#,†,§ NOEL D. LAZO,#,⊥ GAL BITAN,#,† SUMMER BERNSTEIN,|| THOMAS WYTTENBACH,|| MICHAEL T. BOWERS,|| ANDRIJ BAUMKETNER,|| JOAN-EMMA SHEA,|| BRIGITA URBANC,‡ LUIS CRUZ,‡ JOSE BORREGUERO,▽ AND H. EUGENE STANLEY‡

Department of Neurology, David Geffen School of Medicine, Brain Research Institute, and Molecular Biology Institute, University of California, Los Angeles, California 90095, Department of Chemistry and Biochemistry, University of California, Santa Barbara, California 93106, Center for Polymer Studies, Department of Physics, Boston University, Boston, Massachusetts 02215, and Center for the Study of Systems Biology, School of Biology, Georgia Institute of Technology, Atlanta, Georgia 30318

Received March 29, 2006

ABSTRACT

Oligomeric, neurotoxic amyloid protein assemblies are thought to be causative agents in Alzheimer's and other neurodegenerative diseases. Development of oligomer-specific therapeutic agents requires a mechanistic understanding of the oligomerization process. This is a daunting task because amyloidogenic protein oligomers often are metastable and comprise structurally heterogeneous populations in equilibrium with monomers and fibrils. A single methodological approach cannot elucidate the entire protein assembly process. An integrated multidisciplinary program is required. We discuss here the synergistic application of *in hydro*, *in vacuo*, and *in silico* methods to the study of the amyloid β-protein, the key pathogenetic agent in Alzheimer's disease.

1. Introduction

The amyloid β-protein (Aβ) is a peptide that is ubiquitously and normally expressed in humans predominately in two forms, 40- and 42-amino acids in length (Aβ40 and Aβ42, respectively) (see Lazo et al.[1] for a comprehensive review). Aβ fibrils are the principal protein component of the extracellular deposits (amyloid plaques) characteristic of Alzheimer's disease (AD).

$^{1}DAEFRHDSGYEVHHQKLVFFAEDVGSNKGAIIGLMVGGVVIA^{42}$

Amyloid β-protein (Aβ) Sequence

A strong causal link between Aβ and AD has been established through genetic studies showing that autosomal dominant forms of AD invariably involve increased production of Aβ or an increased Aβ42/Aβ40 concentration ratio. *In vitro* biophysical studies have revealed that Aβ42 forms fibrils at significantly higher rates than does Aβ40. Importantly, Aβ42 self-association produces structures that are more neurotoxic than homologous structures formed by Aβ40. The postulated central role of Aβ in AD has focused therapeutic strategies on the control of Aβ production or self-association.

Aβ fibrils are formed by a small number of stacked, extended, ribbon-like β-sheets, each of which is formed by β-strands arranged perpendicular to the fibril axis. To

* To whom correspondence should be addressed. E-mail: dteplow@ucla.edu.
# David Geffen School of Medicine, University of California, Los Angeles.
† Brain Research Institute, University of California, Los Angeles.
§ Molecular Biology Institute, University of California, Los Angeles.
⊥ Current address: Gustaf A. Carlson School of Chemistry and Biochemistry, Clark University, 950 Main St., Worcester, MA 01610.
|| University of California, Santa Barbara.
‡ Boston University.
▽ Georgia Institute of Technology.

Gal Bitan is an Assistant Professor, Department of Neurology, David Geffen School of Medicine at UCLA. Dr. Bitan's program seeks to develop therapeutic agents for Alzheimer's and other neurologic diseases linked to aberrant protein assembly.

Summer Bernstein is a postdoctoral fellow, Department of Chemistry and Biochemistry, University of California at Santa Barbara. Dr. Bernstein is interested in studying solution conformation retention of proteins upon ionization into the gas phase, including aggregates of amyloid proteins linked to Alzheimer's disease and bovine spongiform encephalopathy (BSE; "Mad Cow disease").

Thomas Wyttenbach is an Associate Research Professor, Department of Chemistry and Biochemistry, University of California at Santa Barbara. His interests include the structure and solvation of biologically interesting systems.

Michael T. Bowers is a Professor of Chemistry, Department of Chemistry and Biochemistry, University of California at Santa Barbara. Dr. Bower's interests include protein misfolding and aggregation, G-quadraplex formation and stabilization by drug candidates, and structural analysis of macromolecules in solvent-free environments.

Andrij Baumketner is a postdoctoral fellow in the Department of Chemistry and Biochemistry, University of California at Santa Barbara. Dr. Baumketner's research interests are in theoretical approaches to problems in chemical and biological physics.

Joan-Emma Shea is an Assistant Professor, Department of Chemistry and Biochemistry, University of California at Santa Barbara. Dr. Shea's interests include developing and applying the techniques of statistical and computational physics to the study of biological problems.

Drs. Brigita Urbanc and Luis Cruz are senior research associates, Department of Physics, Boston University. Their research includes studies of biopolymer systems and involves the development and application of modern methods of statistical mechanics: series, Monte Carlo, and renormalization group.

Jose Borreguero is a postdoctoral fellow at the Georgia Institute of Technology. Dr. Borregueuro's graduate work focused on the computational physics of protein folding and assembly.

H. Eugene Stanley is University Professor; Professor of Physics and Physiology, College of Arts and Sciences; Director, Center for Polymer Studies; and Professor of Physiology and Biophysics, School of Medicine, Boston University. Dr. Stanley's interests include the structure of liquid water, statistical physics, and the computational physics of complex biological systems.

David B. Teplow is a Professor of Neurology and Director of the Biopolymer Laboratory, David Geffen School of Medicine at UCLA. Dr. Teplow's work seeks to interface the physical and biological sciences to facilitate a mechanistic understanding of disease and the subsequent development of rational therapeutic strategies.

Noel D. Lazo is an Assistant Professor of Chemistry and Biochemistry, Clark University, and Adjunct Assistant Professor, Department of Neurology, David Geffen School of Medicine at UCLA. Dr. Lazo's interests include the structural pathobiology of amyloidoses and dermatologic diseases.

10.1021/ar050063s CCC: $33.50
Published on Web 07/22/2006

understand how these complex structures form, we have sought to identify assembly intermediates of decreasing complexity, beginning with fibrils and culminating in the study of the Aβ monomer. In 1997, discovery of the penultimate fibril assembly intermediate, the protofibril, was reported.[2] Relative to mature amyloid fibrils, which commonly are observed as long (micrometer length), straight, unbranched filaments of diameter ~10 nm, protofibrils are short (≤150 nm), flexible, narrow (5 nm) assemblies that often have a beaded morphology. Importantly, protofibrils are potent neurotoxins.[3] Continuing *in vitro* studies have revealed ever-smaller Aβ assemblies, all of which are neurotoxic.[4]

An increasing recognition of the biological importance of small Aβ assemblies has come through studies in animals and humans. Evaluation of neuronal function in transgenic mice expressing Aβ has revealed neurological deficits prior to amyloid deposition, suggesting that "soluble" Aβ assemblies were neurotoxic. Subsequent studies in humans have shown that oligomeric forms of Aβ are detectable in the brain and cerebrospinal fluid and that the levels of one type of oligomer, termed Aβ-derived diffusible ligands, are an order of magnitude higher in AD patients than in age-matched controls. These results support the hypothesis that Aβ oligomers are the proximate neurotoxins in AD.[5]

If the oligomer hypothesis is true, development of therapeutic agents would be facilitated by a mechanistic understanding of Aβ monomer folding and oligomerization. Ironically, the *process* of oligomerization interferes with the *study* of oligomerization. In any solution population of Aβ, monomers exist in different conformational states. At Aβ concentrations at which binary or higher-order collisions occur in an experimentally observable time regime, conformational complexity is increased by monomer self-association, which produces a mixture of metastable, noncovalently associated oligomeric assemblies that eventually form fibrils. This makes the use of spectroscopic techniques that yield population-average data, including CD, FT-IR, or NMR, problematic. The noncovalence of the oligomer state prevents oligomer fractionation and quantitation through SDS−PAGE because of SDS-induced dissociation.[6] Aβ has not been crystallized, precluding the use of X-ray diffraction methods. How then does one understand the initial phases of Aβ folding and assembly? We posit that solution of the Aβ assembly problem requires multiple disciplines and the contemporaneous integration of results produced from them. We discuss here our combination of *in hydro*, *in vacuo*, and *in silico* approaches and how this combination has provided insights into the Aβ assembly problem that heretofore were unobtainable.

2. *In Hydro* Studies

In hydro studies of pure populations of full-length Aβ peptides are seminal because they allow determination of intrinsic features of Aβ assembly without confounding variables associated with *ex vivo* (e.g., plasma, cerebrospinal fluid, or brain homogenates) or *in vivo* (neuronal) Aβ preparations. *In hydro* studies provide a standard to which results of high-resolution, non-population-based (single-molecule or oligomolecular) methods, such as mass spectrometry or computational physics, may be compared and thus validated.

2.1. Determining the Aβ Oligomer Size Distribution. Following earlier work defining protofibrillar intermediates[2,3] (section 1), we sought to determine whether pre-protofibrillar, nonmonomeric intermediates existed. To do so, we employed the method of photoinduced cross-linking of unmodified proteins (PICUP) to "freeze" particular equilibrium states of Aβ.[7] PICUP covalently stabilizes oligomers in solution, allowing quantitative determination of the oligomer size distribution using techniques including SDS−PAGE and size exclusion chromatography (SEC). PICUP was used to determine the initial oligomerization states of Aβ40 and Aβ42 (Figure 5, inset). Aβ42 formed pentamer/hexamer units ("paranuclei", blue arrowhead) that self-associated to form higher-order, protofibril-like oligomers (green arrowhead). Aβ40 did not form paranuclei but rather existed as a mixture comprising predominately monomer, dimer, trimer, and tetramer.[8] The unique ability of Aβ42 to form paranuclei offered an explanation for its strong linkage to AD.[8]

2.2. Probing Nucleation of Aβ Monomer Folding. The discovery of a quantized Aβ42 size distribution suggested that some quasi-stable conformation must exist; otherwise a probabilistic distribution of oligomer sizes would have been observed. Secondary structure analyses have shown that monomeric Aβ is largely, but not entirely, disordered, and a quasi-stable monomer fold has been reported in solution-state NMR studies.[9] Aβ oligomerization thus may involve pre-existent folds or monomer folding processes occurring contemporaneously with peptide self-association. To examine this question, we coupled the techniques of limited proteolysis and mass spectrometry. This approach has proven useful in the study of conformational changes in proteins that have a strong propensity to aggregate. Brief endoproteolysis is done under nondenaturing conditions at low enzyme/substrate ratios. Peptide mapping reveals protease-resistant protein segments that by inference must exist in the protein interior or possess stable folds. Using a panel of seven endoproteinases, we defined the temporal order of cleavages within monomeric Aβ40 and Aβ42.[10] Four important results emerged: (1) the cleavage sites of both peptides were identical within the region Asp1−Val39; (2) the Val39−Val40 peptide bond was labile in Aβ40 but not in Aβ42; (3) the Val40−Ile41 peptide bond in Aβ42 was protease sensitive only under denaturing conditions; (4) a contiguous ten-residue region extending from Ala21 to Ala30 was protease resistant in both peptides.

Observations 1−3 have relevance to and are consistent with the fact that the longer Aβ alloform, Aβ42, is linked particularly strongly to AD. Both alloforms have identical primary structure within the Asp1−Val40 region; thus it would be reasonable to predict that identical folding could

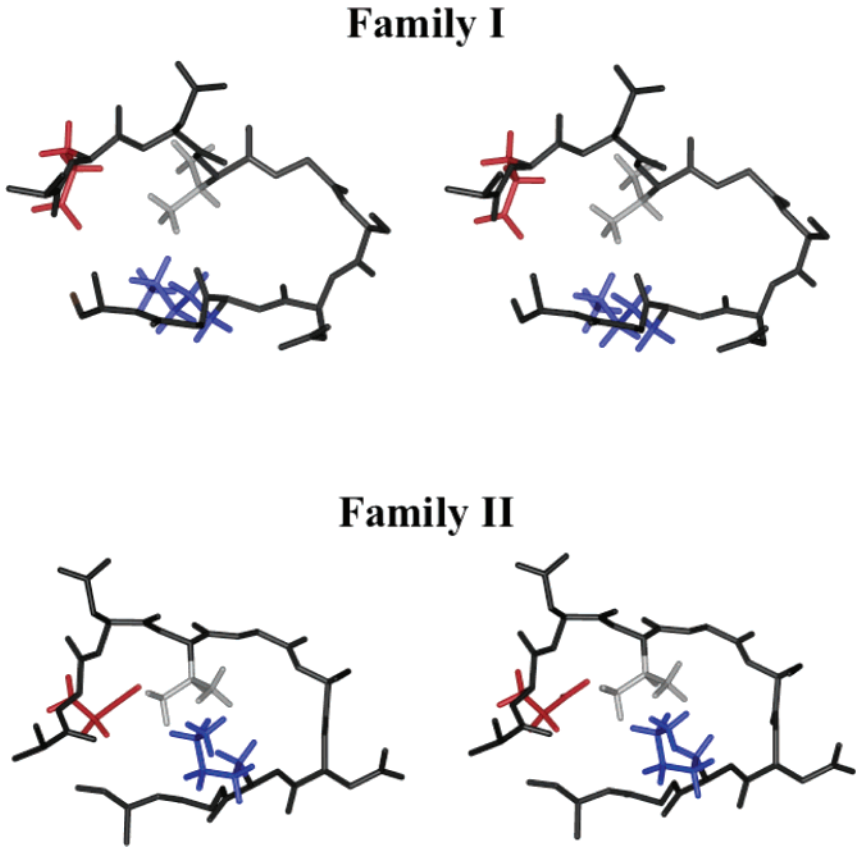

FIGURE 1. Stereoviews of NMR-derived structural models of Aβ(21−30). Heavy-atom representations are shown with Glu22 (red), Val24 (gray), and Lys28 (blue) highlighted. Other atoms are black. All structures display a main chain turn at Val24−Lys28 and a relatively ordered N-terminus. The two families differ in the orientation of the Lys28 side chain.

occur within this region, producing identical results in peptide mapping studies. Identical cleavages were observed within the first 39 residues.[10] In contrast, differences in protease sensitivity might be observed if the Ile41−Ala42 dipeptide contributed to formation of an Aβ42-specific fold involving the peptide C-terminus. Observations 2 and 3 are consistent with the existence of such a postulated fold.

The observation (no. 4) that the Ala21−Ala30 region in both Aβ peptides was protease-resistant suggested that this region was structured and might be the folding nucleus of the Aβ monomer.[10] Peptidic forms of the folding nuclei of some globular proteins have been found to be stable and possess the same structure found in the cognate full-length protein. Indeed, we found that the Aβ-(21−30) decapeptide displayed protease resistance identical to that of full-length Aβ.[10] To determine the structure of Aβ(21−30), solution-state NMR studies were performed, yielding a structural model in which a primary motif was a turn formed by residues Val24-Gly25-Ser26-Asn27-Lys28 (Figure 1). The turn was stabilized by long-range Coulombic interactions between Lys28 and either Glu22 or Asp23 and hydrophobic interaction between the isopropyl and *n*-butyl side chains of Val24 and Lys28, respectively. The intrinsic propensity of the glycine-serine-asparagine residues to be involved in β-turns also could contribute to the favorable energetics of turn formation in the Val24−Lys28 region. These data supported a hypothesis that turn formation nucleated the intramolecular folding of the Aβ monomer. Interestingly, amino acid substitutions at Glu22 and Asp23 are linked to familial forms of AD and cerebral amyloid angiopathy.[1] The turn model suggests that these substitutions cause disease through direct effects on Aβ monomer nucleation.

3. *In Vacuo* Studies

The approaches discussed in sections 2.1 and 2.2 provided valuable information about low-order oligomerization and population-average monomer structure. However, PICUP is not 100% efficient, and therefore it progressively underrepresents oligomer frequency as order increases. Higher-order oligomers are unresolvable by SDS−PAGE. Limited proteolysis identifies flexible versus folded domains but reveals little about *fold structure*. A method able to determine oligomer size at high resolution in complex mixtures and to integrate with computational techniques of structure determination is ion mobility spectrometry (IMS).[11] IMS can be conceptualized as an *in vacuo* analogue of SEC or gel electrophoresis, methods in which molecules of different size, under the influence of a constant fluid flow or electric field (*E*), respectively, move through matrices of defined porosity at different rates. In IMS, the matrix is helium gas in a drift tube. In the tube, ions are accelerated by a constant *E* and decelerated by collisions with He. The result is a constant drift velocity,

v_D, that depends on E and a mobility constant K, according to eq 1.

$$v_D = KE \tag{1}$$

E and mass spectrometer geometry are known; therefore measurement of ion arrival time at the detector determines v_D and, in turn, K. The special value of the IMS approach for studies of protein structure and assembly emanates from the dependence of K on the parameter σ, the [ion] collision cross section (the IMS equivalent of a Stoke's radius in gel permeation chromatography). This relationship is expressed in eq 2.

$$K = \frac{3q}{16N}\left(\frac{2\pi}{\mu k_B T}\right)^{1/2}\frac{1}{\sigma} \tag{2}$$

Here q is ion charge, N is number density of helium gas, μ is reduced mass of the ion−neutral (He) complex, k_B is Boltzmann's constant, and T is temperature. *Because σ depends on the shape of the ion and oligomer order, it is a key experimental constraint in computational modeling of ion structure (section 4.2).*

The most powerful feature of IMS is its ability to resolve ions of different mass m but identical m/z values, where z is charge. These ions are typical of amyloid assembly, in which homotypic self-association/dissociation can be described by eq 3,

$$M^q + nM^q \leftrightarrow M_{(n+1)}^{(n+1)q} \tag{3}$$

where a variable number n of monomers, each of mass M and charge q, add to an initial monomer to produce an oligomer of order $n + 1$ carrying a charge $(n + 1)q$. A dimer M_2 of charge $2q$ and a trimer M_3 of charge $3q$ have m/z values identical to that of the monomer M^q; thus their mass spectra are identical, that is, their peaks are superimposed. However, in IMS,[11] proteins almost always obey the relationship $\sigma_n < n\sigma$, where σ_n is the collision cross section of an nth-order oligomer. For example, σ_{dimer} is almost always smaller than $2\sigma_{monomer}$. Oligomers of identical m/z but different m, contributing to the same peak in the mass spectrum, thus can be resolved in the IMS experiment. The combination of MS and IMS allows determination of oligomer mass and shape and studies of self-association kinetics. In addition, thermodynamic characteristics of monomer and oligomer states can be examined in two ways, by the dependence of the arrival time on injection energy (through collision-induced decomposition (CID)) or temperature (Arrhenius analysis).

3.1. Monitoring Aβ Oligomerization. Bernstein et al.[12] have shown that mass spectrometry of Aβ42 yields peaks with z/n of −4, −3, and −2 (Figure 2). Analysis indicates the −4 and −3 peaks come primarily from monomer ($n = 1$) but the −2 peak comprises predominately oligomers ($n > 1$). In addition, a z/n peak of $-5/2$ is observed. This noninteger value indicates that the ions producing this peak are dimers or higher-order forms of Aβ. To characterize these multimers, the peak of $z/n = -5/2$ was mass-selected and studied by IMS. Arrival time distributions (ATDs) were acquired using three different source acceleration voltages, producing three different injection energies, 23, 50, and 100 eV. Collision of ions with He atoms can produce energy-dependent conformational rearrangements of the ion to a more stable state, or in the case of multimeric species, ion dissociation. As shown in Figure 3c, relatively high injection energy (100 eV) yields an ATD with a major peak centered at ∼600−650 μs, a shoulder at ∼580 μs, and a minor peak centered at ∼350 μs. Because the selected ions were multimeric, it is reasonable to assign the dimer (D) state to the peak at ∼600−650 μs and expect that the shoulder and smaller, earlier peaks will contain higher-order species (section 3).

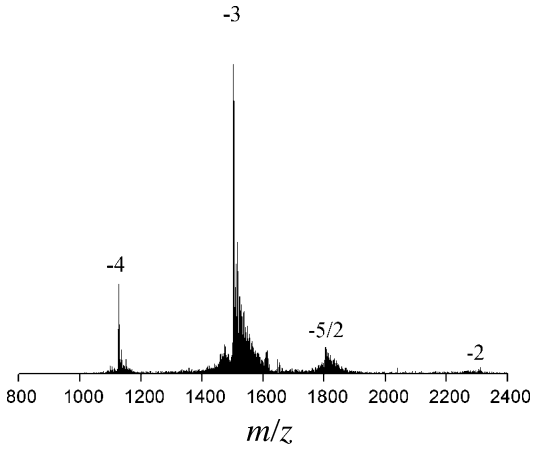

FIGURE 2. Negative ion mass spectrum of Aβ42. The z/n values of the peaks are indicated.

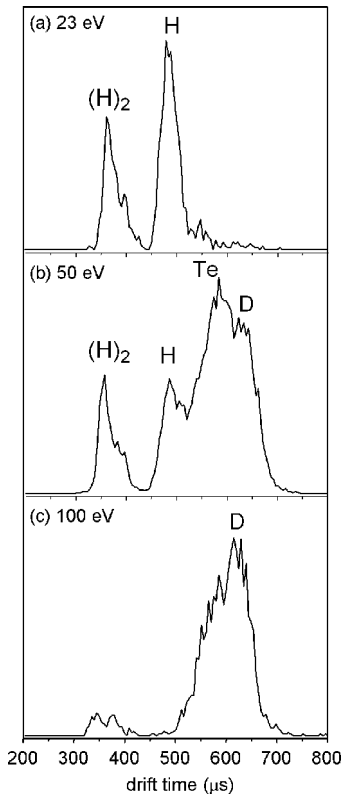

FIGURE 3. Collision-induced decomposition of Aβ42 oligomers. ATD for the $z/n = -5/2$ ion are shown with injection energies indicated. Letters designate dimer (D), tetramer (Te), hexamer (H), and dodecamer ($(H)_2$).

Examination of the data at 50 eV (Figure 3b) is consistent with this expectation. Here three peaks clearly are visible at longer arrival times, at approximately 650, 580, and 480 μs. Beginning with the previously assigned −5 dimer at 650 μs, we assign the peak at 580 μs as the −10 tetramer (Te) and the peak at 480 μs as the −15 hexamer (H). The minor peak at 350 μs observed at 100 eV has a substantial magnitude and is assigned to the −30 dodecamer (H_2). At low (23 eV) injection energy, little dissociation is observed (Figure 3a). The predominant ions are the hexamer (~580 μs) and the dodecamer (~360 μs).

The observation of hexamer and dodecamer at low injection energies is significant for a number of reasons: (1) it suggests that IMS may overcome two major problems in understanding Aβ oligomerization, determining the oligomer size distribution quantitatively and monitoring changes in the distribution contemporaneously with higher-order assembly processes; (2) the identification of paranuclei by IMS−MS, a "noninvasive" approach without the chemical bias of PICUP, suggests that PICUP data for low-order oligomers are an accurate reflection of the oligomerization state; (3) observation of a hexamer ↔ dodecamer equilibrium by IMS and PICUP supports the hypothesis that paranuclei form due to the natural propensity of the Aβ42 peptide to self-associate in a specific manner and that paranuclei assemble homotypically, not by monomer addition; (4) time-dependent formation of paranuclei[8] and higher-order "oligo-paranuclei" have been observed by IMS−MS (Bernstein, S., in preparation), showing that study of the structural factors controlling oligomerization (section 2.2) and the effects of potential therapeutic agents on the process is feasible.

3.2. Thermodynamics of [Pro19]Aβ42 Oligomerization. In IMS, the drift environment is thermal, which allows measurement of the temperature dependence of gas-phase ion reactions that alter σ. If the rates k of these reactions obey the Arrhenius relationship, $k = A\ e^{-E_A/k_BT}$, in which k_B is Boltzmann's constant and T is temperature, the activation energy E_A and the preexponential factor A can be determined. Recently, Bernstein et al.[12] reported studies of [Pro19]Aβ42, an Aβ42 alloform containing a single amino acid substitution in the "central hydrophobic cluster" (CHC) region of the peptide, a region shown to be critical in the initiation and control of peptide assembly.[13] [Pro19]Aβ42 displays limited high-order association relative to wild-type Aβ42,[14] and IMS−MS experiments showed that this peptide forms monomers, dimers, trimers, and tetramers but not hexamers (paranuclei) or higher-order assemblies.[12] Importantly, injection energy studies showed that ions comprising the $-5/2$ charge state underwent dimer (D) ↔ tetramer (Te) transitions amenable to Arrhenius-type investigation. As seen in Figure 4c, D and Te exist in similar amounts at 300 K. With increasing temperature (Figure 4a,b), tetramer dissociation is evident. At higher temperature (440−510 K), dimer dissociation is observed (data not shown). Arrhenius analysis of the temperature dependence of the tetramer (k_1) and dimer (k_2) dissociation rates for the reaction $\text{Te} \xrightarrow{k_1} \text{D} \xrightarrow{k_2} \text{M}$ yielded tetramer and dimer activation energies of dissociation of 18.3 and 20.4 kcal/mol, respectively.[12] It is noteworthy that the E_A values determined by IMS−MS are similar to the 23 kcal/mol energy determined *in hydro* in quasielastic light scattering studies of Aβ40 monomer addition to the growing tip of the amyloid fibril.[15] Two different methods thus suggest the same thing: substantial conformational rearrangement of the Aβ monomer is required for oligomerization and fibril elongation.

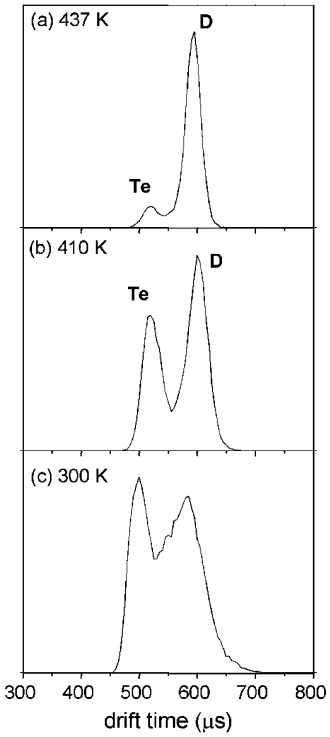

FIGURE 4. Temperature dependence of [Pro19]Aβ42 multimer dissociation. ATD for the $z/n = -5/2$ ion determined at an injection energy of 40 eV at the designated temperatures. Letters designate dimer (D) and tetramer (Te).

4. *In Silico* Studies

In developing therapeutic agents for human diseases, it is useful to determine a target structure at atomic resolution. One of the most powerful methods to do so is computational (*in silico*) physics, the study of physical systems simulated in computers. In simulations of protein folding and self-association, the positions of every atom are known at each step, allowing determination of secondary, tertiary, and quaternary structure. Importantly, the effects of alterations in primary structure or simulation milieu (e.g., solvent polarity) can be determined. The *in silico* approach providing the most detailed information is "all-atom" molecular dynamics (MD) with explicit solvent. Here, all protein atoms are considered along with thousands of water molecules. Monitoring the positions and forces among thousands of atoms simultaneously and continuously is computationally demanding; thus the all-atom MD approach is limited to time regimes of <1 μs.[16] However, biologically relevant protein folding and association processes occur within a broad time regime

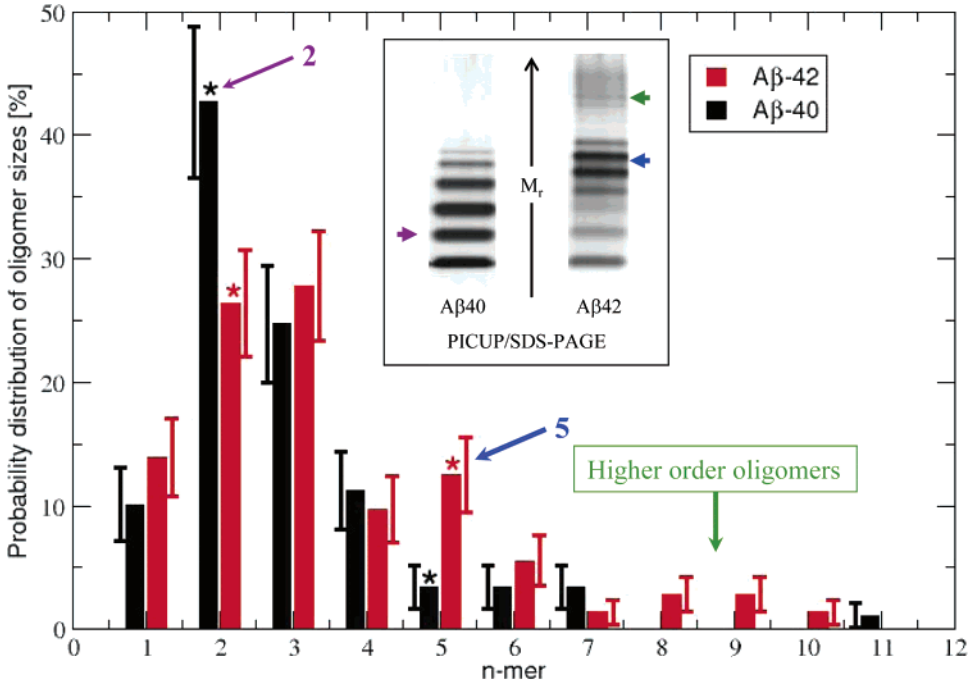

FIGURE 5. Aβ oligomer distributions. Frequency distributions for monomers and higher-order oligomers of Aβ40 (black) and Aβ42 (red) were obtained by averaging over DMD simulation time frames of 9.0, 9.5, and 10.0 million steps. Vertical bars indicate standard errors. Asterisks ($*$) indicate statistically significant ($p < 0.05$) frequency differences between Aβ40 and Aβ42. The inset shows PICUP analysis of Aβ oligomerization: apparent molecular weight, M_r; dimer band, purple arrow; pentamer/hexamer band, blue arrow; dodecamer band, green arrow.

extending from milliseconds to days. To enable study of these "slow" processes, system simplifications are necessary. These have included protein models in which various groups of atoms (e.g., N−H, C═O, $(CH_2)_4-NH^+_3$) are replaced by single beads, the elimination of solvent water through its implicit consideration within the force equations governing interbody interactions, and the development of accelerated methods for sampling conformational space. These latter methods include discrete MD (DMD) and replica-exchange MD (REMD), used for simulations of molecular ensembles or single molecules, respectively. Combining DMD with simplified protein models and implicit solvent[17−24] can increase simulation speeds by a factor of $\sim 10^7$ and allow study of large systems (potentially up to 100 proteins). In the DMD approach, the simplifications that make this approch so efficient also can introduce inaccuracies. For example, the use of a simplified protein model (side chains are represented by single beads) and a coarse-grained force field may result in the neglect of side chain−side chain interactions that contribute to Aβ folding and aggregation. The use of implicit solvent means that the forces operating in solvent-accessible regions (protein surfaces) are the same as those in solvent-inaccessible regions (protein or aggregate interiors). This is not the case biologically or when explicit solvent is included. However, because simulation methods are flexible, limitations such as these can be diminished at some cost to efficiency. In the REMD technique, multiple simulations (replicas) of the system at different temperatures are performed in parallel. After a selected number of MD steps, two replicas are swapped with a probability that depends on the potential energy and temperature differences between them. The simulations then are continued, and many additional swaps are performed. This process has been shown to efficiently sample the conformational space of peptides and small proteins and reveal low-energy conformations.[25,26]

4.1. DMD Simulations of Aβ40 and Aβ42 Oligomerization. *In hydro* (section 2) and *in vacuo* (section 3) studies of Aβ oligomerization support the hypothesis that Aβ40 and Aβ42 fold and oligomerize distinctly. To examine these processes at the atomic level, DMD experiments were performed with implicit water using a simplified (four-bead) protein model.[27] The model represents the backbone atoms using a single bead for the amide NH, the $C_\alpha H$, and the C═O group. A fourth bead represents the amino acid side chain and is placed at the position of the C_β carbon. Glycine has only three beads. Hydrophobic "attraction" and hydrophilic "repulsion" between pairs of side chains are implemented using an experimentally-determined hydropathy scale. The simulations comprised eight systems of 32 Aβ40 monomers each and eight systems of 32 Aβ42 monomers each. The initial conformers displayed zero average potential energy and lacked α-helical or β-strand structure. After 10^7 simulation steps, oligomer frequency distributions were determined for each trajectory and averaged for each Aβ alloform (Figure 5). Four important features were observed: (1) the distributions of Aβ40 and Aβ42 were distinct; (2) the Aβ40 distribution was characterized by a single peak at dimer and a monotonic decrease of frequencies of higher-order oligomers; (3) the Aβ42 distribution had one peak near

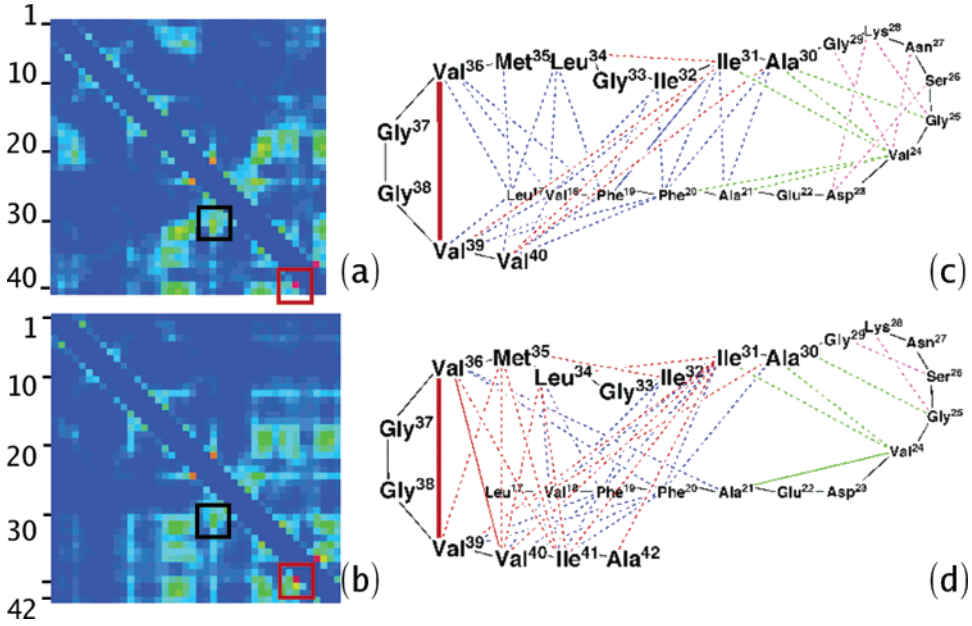

FIGURE 6. Intramolecular contact maps in Aβ pentamers for Aβ40 (a and c) and Aβ42 (b and d). In panels a and b, bimolecular contacts are shown (one peptide N-terminus is at the top left and the other is at the bottom left). Contact strength is indicated spectrally from blue (none) to red (strong). In panels c and d, contacts and their strengths are indicated by dotted (weak), thin solid (moderate), and thick solid (strong) lines.

trimer and a second near pentamer; (4) the Aβ42 distribution included significant levels of high-order oligomers.

The simulation data correlate well with those of PICUP experiments (see Figure 5 (inset) and section 2.1). Low-order ($n \leq 4$) Aβ40 oligomer frequencies are substantially higher than those of larger oligomers, and a maximum in the distribution occurs at dimer/trimer (Figure 5, purple arrow and arrowhead). The Aβ42 distribution has a maximum at pentamer/hexamer (Figure 5, blue arrow and arrowhead). Importantly, the differences between frequencies of dimers and pentamers in Aβ40 and Aβ42 are statistically significant. Experimental data (Figure 5, inset) show higher-order Aβ42 oligomers but no equivalent Aβ40 oligomers. A similar observation is apparent in the simulation (Figure 5, green arrow and arrowhead). The simulation results do not duplicate the PICUP results in every detail. This is not surprising considering the simplified protein model and force parameters incorporated into the simulation. The data do emphasize how well a simplified DMD simulation models the *in hydro* reality.

In addition to providing data on oligomerization *per se*, the simulations allowed construction of "contact maps," two-dimensional arrays representing the contact frequencies of pairs of amino acids. Urbanc et al.[27] studied both intra- and intermolecular contacts for Aβ40 and Aβ42 monomers and oligomers. Results of analyses of contacts in Aβ monomers within pentamers are informative (Figure 6). The addition of two amino acids at the peptide C-terminus significantly increases the number of contacts (cf. Figure 6, panels c and d). These additional contacts do not involve only the isoleucine−alanine residues but result from the involvement of residues in the 1−40 region establishing contacts where none existed before. In particular, Met35 contacts the Aβ C-terminus in Aβ42 but not in Aβ40. Experimental studies have shown that oxidation of Met35 blocks paranucleus formation as well as fibrillogenesis,[28] likely due to the high energetic cost of burying the polar oxidized forms of the Met35 side chain in a hydrophobic cluster involving the Aβ C-terminus and CHC. The Met35 contacts revealed through simulation offer a high-resolution "view" of these interactions. In addition, they identify amino acids whose structural modification would be predicted to alter folding and oligomerization, predictions that are testable experimentally.

4.2. REMD Simulations of Aβ42 Folding. Proper interpretation of IMS spectra requires structural modeling of the ions examined.[11] Baumketner et al.[25] now have reported models of Aβ42 ions investigated by IMS (section 3). To do so, REMD experiments were done in implicit water or in a solvent-free (sf) milieu. A third population was obtained by computationally dehydrating the conformers simulated in implicit water. Figure 7 presents scatter plots of the calculated σ values for members of each population (a−c), along with experimentally observed (d) and theoretical (e) ATDs. It is noteworthy that the calculated $\bar{\sigma}_{\text{dehydrated}}$ and $\bar{\sigma}_{\text{sf}}$ values agree within 10% with the experimentally determined absolute σ values corresponding to the two peaks in the ATD (Figure 7, dotted vertical lines). Dehydration of fully solvated analytes occurs in the source of the IMS instrument, and thus the agreement between σ values for the computationally and physically dehydrated conformers (cf. Figure 7, panels b and d) is likely to be biophysically relevant. Similarly, a dehydrated molecule in the gas phase, a highly nonpolar environment, also could fold into a compact structure in which apolar groups are exposed to the "solvent" (vacuum) and polar groups are sequestered in the interior. Such sf

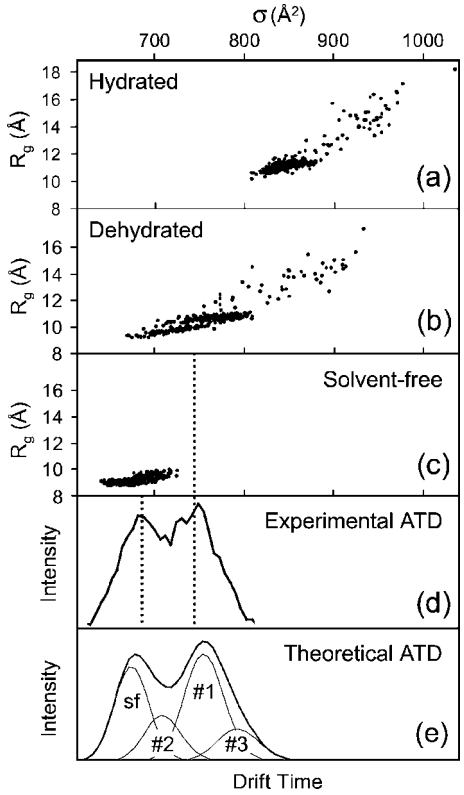

FIGURE 7. Correlation of Aβ42 REMD and IMS data. Scatter plots of radius of gyration (R_g) versus σ are shown for peptide conformers in (a) hydrated, (b) dehydrated, and (c) sf forms. Panel d shows the experimentally determined Aβ42 ATD. Panel e shows the simulated ATD.

structures and their mirror-image "aqueous" equivalents were observed experimentally and computationally (cf. panels c and d, Figure 7).

To determine whether discrete structural families existed within the population of dehydrated conformers, principal coordinate and principal component analyses, computational methods for clustering structurally related conformers, were done.[25] Three similar clusters (C1−C3) were revealed by each approach. Each had similar average potential energy, highlighting the fact that Aβ42 can adopt many different low-energy conformations. Importantly, the experimentally determined ATD could be modeled quite accurately assuming it comprised structures from clusters sf and C1−C3 (Figure 7e). Determination of residue-specific secondary structure revealed that each cluster had distinct secondary structure distributions and no cluster possessed >10−20% α- or β-structure. This result was consistent with experimental data showing that freshly prepared Aβ is largely disordered in aqueous solution.[29] The ability of REMD to reproduce experimentally observed σ values and secondary structure features in low-energy Aβ42 clusters suggests that expanded REMD studies of Aβ42-folding dynamics will be informative and relevant.

4.3. Folding of Aβ(21−30). 4.3.1. DMD Simulation. The earliest event in Aβ self-assembly is monomer folding. To study this process at high resolution, Borreguero et al.[30] used DMD and a "united-atom" protein model (specifying

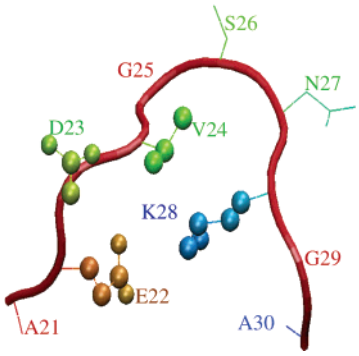

FIGURE 8. Structure of Aβ(21−30). A representative conformer with the united-atom "balls" of Glu22, Asp23, Val24, and Lys28 is shown. Backbone atoms are indicated by a red tube.

all atoms except hydrogens). Hydrogen bonding, electrostatic interactions, and solvent effects (implicit through hydropathic interactions) were implemented. Trajectories were produced at six different electrostatic interaction (EI) strengths, including those appropriate for cytoplasmic/extracellular (aqueous; low EI) or membrane (lipid; high EI) milieus. Trajectories at zero EI strength were produced to account for a milieu in which electrostatic interactions are completely shielded by the solvent and to determine a relative contribution of EI to folding in other milieus. A representative structure from the simulations is shown in Figure 8. Key features include a global turn organization, hydrophobic interaction between the isopropyl side chain of Val24 and the *n*-butyl side chain of Lys28, electrostatic interactions between the N_ϵ group of Lys28 and the carboxylates of Glu22 and Asp23, and a lack of backbone hydrogen bonds. Trajectories with nonzero EI displayed compaction of relatively extended conformers with concurrent decreases in the solvent-accessible surface area (SASA) and $C_\alpha-C_\alpha$ distances of Val24 and Lys28. Hydrophobic interactions were the primary force driving turn formation. Electrostatic interactions stabilized the turn. These observations were consistent with experimental[10] (section 2.2) and computational[27] (section 4.1) results. The EI-dependence of turn structure was illuminating. The Lys28 side chain "flipped" from one side of the plane of the turn to the other, depending on EI. At low to moderate EI, Lys28−Glu22 electrostatic interactions were favored. At higher EI, the Lys28 side chain flipped to the other side of the turn, favoring Lys28−Asp23 interactions. The latter interaction has been shown to occur in fibrils. The data predict that mutations destabilizing Glu22−Lys28 interactions or stabilizing Asp23−Lys28 interaction could facilitate fibril formation and thus be pathogenic. With respect to the latter point, Sciarretta et al. have shown that covalent cross-linking (lactam formation) between Lys28−Asp23 eliminates the lag phase in fibril formation and increases the fibril formation rate by a factor of ∼1000.[31] In fact, all human disease-causing mutations affecting the Ala21−Ala30 region of Aβ appear to alter the stability of the turn (Grant et al., in preparation).

4.3.2. All-Atom MD Simulation. The relatively small number of atoms in the Aβ(21−30) system made it amenable to all-atom MD simulations in explicit water.

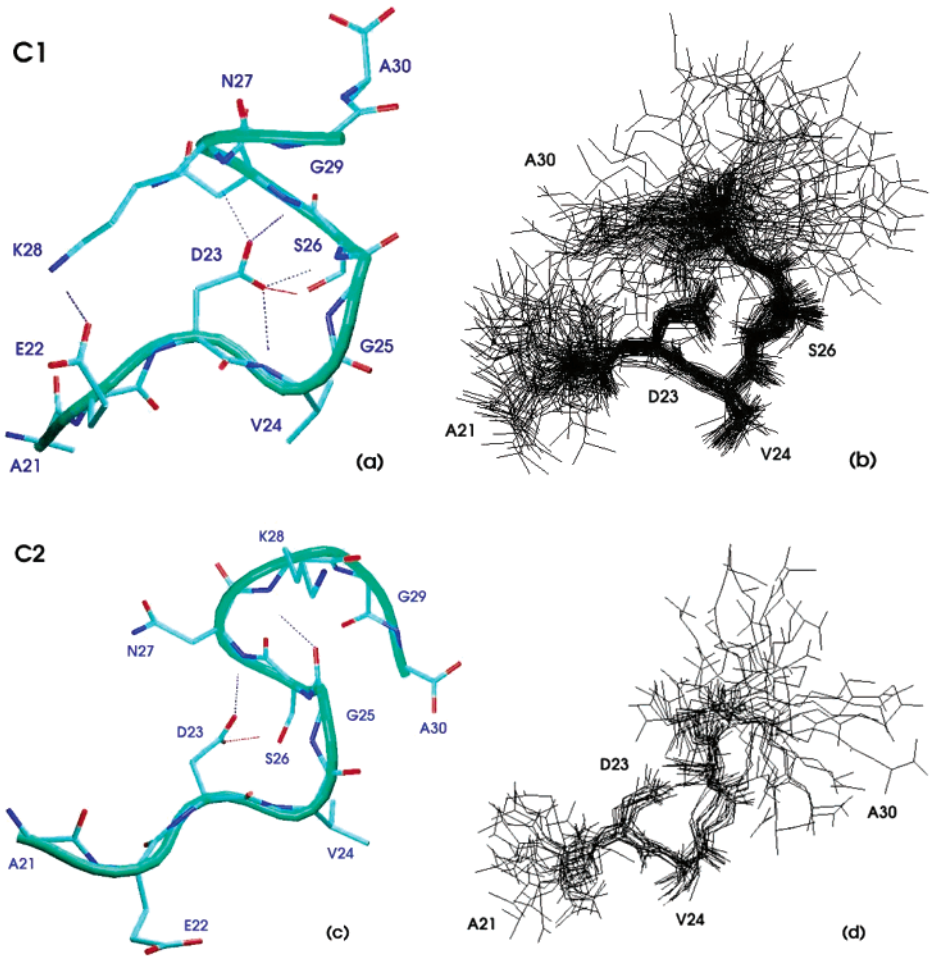

FIGURE 9. Conformations within clusters C1 (a and b) and C2 (c and d). Centroids of the clusters are shown in panels a and c. Superimpositions of conformers are shown in panels b and d.

Cruz et al.[32] simulated five folding processes: (1) wild type (WT) Aβ(21−30) in "random coil" (RC) conformation; (2, 3) the average family I and II turn structures from Lazo et al.[10] (Figure 1) in reduced density water; (4) Aβ(21−30) containing the Glu22 → Gln "Dutch" substitution; (5) WT peptide in high ionic strength water (containing NaCl). In all five trajectories, the conformers displayed relatively rigid turns with highly flexible termini, as seen experimentally in prior NMR studies.[10] Hydrophobic events, characterized by packing of the Val24 isopropyl side chain with the Lys28 *n*-butyl side chain, predominated over electrostatic interactions involving the side chains of Glu22, Asp23, and Lys28. For the WT peptides, the hydrophobic and electrostatic interactions occurred simultaneously frequently (>70% of the time), consistent with the suggested stabilizing role of electrostatics.[10] An observation highlighting the ability of single-molecule methods (*in silico* techniques) to reveal interactions that averaging methods (NMR among others) cannot is that of a periodic, close (<4.2 Å) contact (salt-bridge) involving Lys28 and either Glu22 or Asp23. NMR studies have revealed only long-range (>9 Å) Coulombic interactions among these residues.[10] In all trajectories except the "NaCl," the Glu22−Lys28 and Asp23−Lys28 electrostatic interactions were mutually exclusive, consistent with the flipping of the Lys28 side chain observed by Borreguero et al.[30] In the trajectory with NaCl, contemporaneous Glu22−Lys28 and Asp23−Lys28 interactions and Val24−Lys28 packing were observed, possibly due to salt effects on peptide−water hydrogen bonding.

4.3.3. REMD Simulation. All-atom REMD with explicit solvent also has been applied to the Aβ(21−30) folding problem.[26] Two structural clusters were observed with occurrence frequencies ≥5%, C1 (30%) and C2 (10%). C1 occupied the global minimum on the free energy surface and C2 occupied a local minimum. The thermodynamic stability of these clusters suggested that their component conformers were biophysically relevant. Figure 9 shows the most representative conformation from C1 (panel a) and a superimposition of C1 conformers (panel b) to illustrate conformational variability. A stable core involving Glu22−Lys28 and displaying a bend between Val24 and Lys28 was observed. Lys28(N_ζ)−Glu22(C_δ) distance measurements revealed two maxima (3.4 and 6.3 Å), suggesting the existence of short-range (salt-bridge) and long-range (water-mediated) Coulombic interactions. One long-range (~6.5 Å) interaction was seen between Lys28(N_ζ) and Asp23($C\gamma$) atoms. Interestingly, strong hydrogen bonds were noted between Asp23(O_δ) and Gly25, Ser26, Asn27, and Lys28. Hydrogen bonds were not seen by

NMR,[10] possibly because the spectra are ensemble averages of peptide structures. C2 conformers also possess a bend (Figure 9, panels c and d), but the Glu22−Lys28 salt bridge is absent, and hydrogen bonding patterns differ significantly. An important difference between C1 and C2 is the position of the Lys28 side chain, which exists on opposite sides of the bend plane in the two clusters, as observed in NMR studies.[10]

A novel result of the REMD studies is insight into the unusual protease resistance of Aβ(21−30). One can compare C1 conformer structures to significantly (C_α RMSD >1 Å) divergent structures in other clusters. Divergent conformers can be considered higher energy, non-native states analogous to denatured conformers, states predicted to have larger radii of gyration, molecular volumes, and SASA. Surprisingly, divergent conformers displayed only modest increases in these parameters (5.1 vs 4.5 Å, 937.9 vs 933.5 Å^2, and 10.6 vs 10.0 Å, respectively), and all possessed the central Val24−Lys28 bend.[26] Thus, in both the lowest-energy "native state" and higher-energy "denatured" states, the Aβ(21−30) peptide maintains its bend topology and overall size. This conformational stability may explain the extraordinary protease resistance of this region of Aβ and its lack of aggregation, consistent with its low propensity to fold into an aggregation-competent conformation.

4.3.4. Simulating Aβ(21−30) Folding: A Synthesis. The greatest uncertainty in *in silico* studies is the level at which they reproduce physical reality. Confidence in the relevance of simulations comes from agreement among studies done using different algorithms and, importantly, from agreement with experiment. The three different Aβ-(21−30) simulation approaches produced a consistent picture of an Ala21−Ala30 fold characterized by a turn or bend structure stabilized by hydrophobic and Coulombic interactions and displaying flexible termini. These structural models were consistent with results of biochemical, mass spectrometric, and NMR experiments (sections 2 and 3). For example, C_α RMSD values between turn region models based on simulation[26,30] and NMR-derived constraints[10] were as low as 0.7−1.1 Å. The remarkable agreement among computational and experimental studies supports the biophysical relevance of the global fold thus determined for the Aβ(21−30) decapeptide.

An important additional observation was that data from the three simulation methods were not entirely identical. This was encouraging because it ruled out the possibility that all the simulations might agree but still be wrong because of the inclusion in each of the same misassumption(s). As an example, only REMD simulations revealed strong hydrogen bonding between Asp23 and other residues within the turn. This observation has stimulated further examination of whether hydrogen bonding may in fact exist within Aβ conformers simulated using DMD and MD or within synthetic peptides in solution. The results thus obtained will strengthen our understanding of Aβ structural biology and improve our simulation algorithms and methods of experimental study.

5. Summary

In hydro, *in vacuo*, and *in silico* methods have been integrated into a coordinated program to understand Aβ self-assembly. The integration allows study of phenomena within broad structural and temporal regimes. *In hydro* experiments reveal relatively gross, population-average features of Aβ monomer folding and oligomerization. These include the roles of turns in nucleating monomer folding and of the C-terminus in mediating oligomerization. IMS can identify/quantify specific oligomer types and produce thermodynamic information about oligomer association. *Ab initio in silico* procedures, constrained by the experimental results, produce biophysically relevant models of monomer and oligomer structure, reveal atomic contacts, elucidate the temporal (thermo)dynamics of folding and self-association, and allow virtual study of milieu-dependent (e.g., membrane or cytoplasm) folding events. Each discipline informs and validates the others, as well as stimulates new experimental and computational questions. Importantly, the paradigm supports studies of other pathologic proteins and can be applied directly in experimental and computational drug discovery.

Strict page limits preclude citation of a large body of excellent work by colleagues in the fields discussed. We acknowledge these efforts here. This work was supported by NIH Grants NS38328, NS44147, AG18921, and AG027818 (D.B.T.), and AG023661 (H.E.S.), NSF Career Award No. 0133504 (J.-E.S.), NSF Grants CHE-0140215 and CHE-0503728 (M.T.B.), and the generosity of the Foundation for Neurologic Diseases (D.B.T.), the A. P. Sloan Foundation (J.-E.S.), the David and Lucile Packard Foundation (J.-E.S.), the Alzheimer's Association (D.B.T. and H.E.S.), and Mr. Stephen Bechtel, Jr. (H.E.S.).

References

(1) Lazo, N. D.; Maji, S. K.; Fradinger, E. A.; Bitan, G.; Teplow, D. B. The amyloid β-protein. In *Amyloid Proteins-The Beta Sheet Conformation and Disease*; Sipe, J. C., Ed.; Wiley-VCH: Weinheim, Germany, 2005; pp 385−492.

(2) Walsh, D. M.; Lomakin, A.; Benedek, G. B.; Condron, M. M.; Teplow, D. B. Amyloid β-protein fibrillogenesis: Detection of a protofibrillar intermediate. *J. Biol. Chem.* **1997**, *272*, 22364−22372.

(3) Walsh, D. M.; Hartley, D. M.; Kusumoto, Y.; Fezoui, Y.; Condron, M. M.; Lomakin, A.; Benedek, G. B.; Selkoe, D. J.; Teplow, D. B. Amyloid β-protein fibrillogenesis: Structure and biological activity of protofibrillar intermediates. *J. Biol. Chem.* **1999**, *274*, 25945−25952.

(4) Kirkitadze, M. D.; Bitan, G.; Teplow, D. B. Paradigm shifts in Alzheimer's disease and other neurodegenerative disorders: The emerging role of oligomeric assemblies. *J. Neurosci. Res.* **2002**, *69*, 567−577.

(5) Klein, W. L.; Stine, W. B., Jr.; Teplow, D. B. Small assemblies of unmodified amyloid β-protein are the proximate neurotoxin in Alzheimer's disease. *Neurobiol. Aging* **2004**, *25*, 569−580.

(6) Bitan, G.; Fradinger, E. A.; Spring, S. M.; Teplow, D. B. Neurotoxic protein oligomers—What you see is not always what you get. *Amyloid* **2005**, *12*, 88−95.

(7) Bitan, G.; Teplow, D. B. Rapid photochemical cross-linking—A new tool for studies of metastable, amyloidogenic protein assemblies. *Acc. Chem. Res.* **2004**, *37*, 357−364.

(8) Bitan, G.; Kirkitadze, M. D.; Lomakin, A.; Vollers, S. S.; Benedek, G. B.; Teplow, D. B. Amyloid β-protein (Aβ) assembly: Aβ40 and Aβ42 oligomerize through distinct pathways. *Proc. Natl. Acad. Sci. U.S.A.* **2003**, *100*, 330−335.

(9) Zhang, S.; Iwata, K.; Lachenmann, M. J.; Peng, J. W.; Li, S.; Stimson, E. R.; Lu, Y.; Felix, A. M.; Maggio, J. E.; Lee, J. P. The Alzheimer's peptide Aβ adopts a collapsed coil structure in water. *J. Struct. Biol.* **2000**, *130*, 130−141.

(10) Lazo, N. D.; Grant, M. A.; Condron, M. M.; Rigby, A. C.; Teplow, D. B. On the nucleation of amyloid β-protein monomer folding. *Protein Sci.* **2005**, *14*, 1581−1596.

(11) Wyttenbach, T.; Bowers, M. T. Gas-phase conformations: The ion mobility/ion chromatography method. In *Topics in Current Chemistry*; Springer: Berlin, 2003; Vol. 225, pp 207−232.
(12) Bernstein, S. L.; Wyttenbach, T.; Baumketner, A.; Shea, J.-E.; Bitan, G.; Teplow, D. B.; Bowers, M. T. Amyloid β-protein: Monomer structure and early aggregation states of Aβ42 and its Pro19 alloform. *J. Am. Chem. Soc.* **2005**, *127*, 2075−2084.
(13) Teplow, D. B. Structural and kinetic features of amyloid β-protein fibrillogenesis. *Amyloid* **1998**, *5*, 121−142.
(14) Bitan, G.; Vollers, S. S.; Teplow, D. B. Elucidation of primary structure elements controlling early amyloid β-protein oligomerization. *J. Biol. Chem.* **2003**, *278*, 34882−34889.
(15) Kusumoto, Y.; Lomakin, A.; Teplow, D. B.; Benedek, G. B. Temperature dependence of amyloid β-protein fibrillization. *Proc. Natl. Acad. Sci. U.S.A.* **1998**, *95*, 12277−12282.
(16) Urbanc, B.; Borreguero, J. M.; Cruz, L.; Stanley, H. E. Ab initio discrete molecular dynamics approach to protein folding and aggregation. *Methods Enzymol.* **2006**, *412*, 314−338.
(17) Zhou, Y.; Hall, C. K.; Karplus, M. First-order disorder-to-order transition in an isolated homopolymer model. *Phys. Rev. Lett.* **1996**, *77*, 2822−2825.
(18) Zhou, Y.; Karplus, M. Folding thermodynamics of a three-helix-bundle protein. *Proc. Natl. Acad. Sci. U.S.A.* **1997**, *94*, 14429−14432.
(19) Zhou, Y.; Karplus, M.; Wichert, J. M.; Hall, C. K. Equilibrium thermodynamics of homopolymers and clusters: molecular dynamics and Monte Carlo simulations of system with square-well interactions. *J. Chem. Phys.* **1997**, *107*, 10691−10708.
(20) Dokholyan, N. V.; Buldyrev, S. V.; Stanley, H. E.; Shakhnovich, E. I. Discrete molecular dynamics studies of folding of a protein-like model. *Folding Des.* **1998**, *3*, 577−587.
(21) Smith, A. V.; Hall, C. K. α-Helix formation: Discontinuous molecular dynamics on an intermediate-resolution protein model. *Proteins* **2001**, *44*, 344−360.
(22) Smith, A. V.; Hall, C. K. Assembly of a tetrameric α-helical bundle: Computer simulations on an intermediate-resolution protein model. *Proteins* **2001**, *44*, 376−391.
(23) Smith, A. V.; Hall, C. K. Protein refolding versus aggregation: Computer simulations on an intermediate-resolution protein model. *J. Mol. Biol.* **2001**, *312*, 187−202.
(24) Ding, F.; Borreguero, J. M.; Buldyrev, S. V.; Stanley, H. E.; Dokholyan, N. V. A Mechanism for the α-helix to β-hairpin transition. *Proteins: Struct., Funct., Genet.* **2003**, *53*, 220−228.
(25) Baumketner, A.; Bernstein, S. L.; Wyttenbach, T.; Bitan, G.; Teplow, D. B.; Bowers, M. T.; Shea, J.-E. Amyloid β-protein monomer structure: A computational and experimental study. *Protein Sci.* **2006**, *15*, 420−428.
(26) Baumketner, A.; Bernstein, S. L.; Wyttenbach, T.; Lazo, N. D.; Teplow, D. B.; Bowers, M. T.; Shea, J.-E. Structure of the 21−30 fragment of amyloid β-protein. *Protein Sci.* **2006**, *15*, 1239−1247.
(27) Urbanc, B.; Cruz, L.; Yun, S.; Buldyrev, S. V.; Bitan, G.; Teplow, D. B.; Stanley, H. E. *In silico* study of amyloid β-protein folding and oligomerization. *Proc. Natl. Acad. Sci. U.S.A.* **2004**, *101*, 17345−17350.
(28) Bitan, G.; Tarus, B.; Vollers, S. S.; Lashuel, H. A.; Condron, M. M.; Straub, J. E.; Teplow, D. B. A molecular switch in amyloid assembly: Met^{35} and amyloid β-protein oligomerization. *J. Am. Chem. Soc.* **2003**, *125*, 15359−15365.
(29) Kirkitadze, M. D.; Condron, M. M.; Teplow, D. B. Identification and characterization of key kinetic intermediates in amyloid β-protein fibrillogenesis. *J. Mol. Biol.* **2001**, *312*, 1103−1119.
(30) Borreguero, J. M.; Urbanc, B.; Lazo, N. D.; Bitan, G.; Buldyrev, S. V.; Teplow, D. B.; Stanley, H. E. Folding events in the 21−30 region of amyloid β-protein (Aβ) studied *in silico*. *Proc. Natl. Acad. Sci. U.S.A.* **2005**, *102*, 6015−6020.
(31) Sciarretta, K. L.; Gordon, D. J.; Petkova, A. T.; Tycko, R.; Meredith, S. C. Aβ40-Lactam(D23/K28) models a conformation highly favorable for nucleation of amyloid. *Biochemistry* **2005**, *44*, 6003−6014.
(32) Cruz, L.; Urbanc, B.; Borreguero, J. M.; Lazo, N. D.; Teplow, D. B.; Stanley, H. E. Solvent and mutation effects on the nucleation of amyloid β-protein folding. *Proc. Natl. Acad. Sci. U.S.A.* **2005**, *102*, 18258−18263.

AR050063S